Stabilization of a Class of Underactuated Mechanical Systems via Interconnection and Damping Assignment

Romeo Ortega
Lab. des Signaux et Systèmes
CNRS-SUPELEC
Gif–sur–Yvette 91192
FRANCE
tel. no:(33)-01-69-85-17-65
fax. no:(33)-01-69-85-17-66
Romeo.Ortega@lss.supelec.fr

Mark W. Spong
Coordinated Science Lab
University of Illinois
Urbana, IL 61801
USA
tel. no:(1)-217-333-4281
fax. no:(1)-217-244-1653
m-spong@uiuc.edu

Fabio Gómez-Estern
Dept. Ing. de Sistemas y Automática
Escuela Superior de Ingenieros
C. de los Descubrimientos, 41092 Sevilla
SPAIN
tel. no:(34)-95-4487361
fax. no:(34)-95-4487340
fgs@cartuja.us.es

Guido Blankenstein
EPFL/DMA MA
Ecublens CH-1015
Lausanne
SWITZERLAND
tel. +41 21 693 4989
fax +41 21 693 5839
guido.blankenstein@epfl.ch

January 9, 2002

Keywords: Underactuated mechanical systems, Hamiltonian systems, nonlinear control, energy shaping, passivity.

Abstract

In this paper we consider the application of a new formulation of Passivity Based Control, known as Interconnection and Damping Assignment, or IDA-PBC, to the problem of stabilization of *underactuated mechanical systems*, which requires the modification of both the potential and the kinetic energies. Our main contribution is the characterization of a class of systems for which IDA-PBC yields a smooth asymptotically stabilizing controller with a guaranteed domain of attraction. The class is given in terms of solvability of certain partial differential equations. One important feature of IDA–PBC, stemming from its Hamiltonian (as opposed to the more classical Lagrangian) formulation, is that it provides new degrees of freedom for the solution of these equations. Using this additional freedom, we are able to show that the method of "controlled Lagrangians"—in its original formulation—may be viewed as a special case of our approach. As illustrations we design asymptotically stabilizing IDA-PBC's for the classical ball and beam system and a novel inertia wheel pendulum. For the former we prove that for all initial conditions (except a set of zero measure) we drive the beam to the right orientation. Also, we define a domain of attraction for the zero equilibrium that ensures that the ball remains within the bar. For the inertia wheel we prove that it is possible to swing up and balance the pendulum without switching between separately derived swing up and balance controllers and without measurement of velocities.

1 Introduction

Passivity–based control (PBC) is a design methodology for control of nonlinear systems which is well–known in mechanical applications. In some regulation problems it provides a natural procedure to shape the *potential* energy preserving in closed–loop the Euler–Lagrange (EL) structure of the system. As thoroughly discussed in [16], PBC is also applicable to a broad class of systems described by the EL equations of motion, including electrical and electromechanical systems. In [17] we proposed the utilization of dynamic EL controllers, coupled with the plant via power–preserving interconnections (hence preserving the EL structure), to shape the potential energy of a class of underactuated EL systems via partial state measurements. It is well known, however, that to stabilize some underactuated mechanical devices, as well as most electrical and electromechanical systems, it is necessary to modify the *total* energy function. Unfortunately, total energy shaping with the classical procedure of PBC, where we first *select* the storage function to be assigned and then design the controller that enforces the dissipation inequality, destroys the EL structure. That is, in these cases, the closed–loop—although still defining a passive operator—is no longer an EL system, and the storage function of the passive map (which is typically quadratic in the errors) is not an energy function in any meaningful physical sense. As explained in Section 10.3.1 of [16], this situation stems from the fact that these designs carry out an inversion of the system along the reference trajectories, inheriting the poor robustness properties of feedback linearizing designs and imposing an unnatural stable invertibility requirement to the system.

To overcome this problem we have developed in [18] (see also [19, 28]) a new PBC design methodology called interconnection and damping assignment or IDA–PBC. The main distinguishing features of IDA–PBC are that: 1) it is formulated for systems described by so–called port–controlled Hamiltonian models, which is a class that *strictly contains* EL models, and 2) the closed–loop energy function is obtained—via the solution of a partial differential equation (PDE)—*as a result* of our choice of desired subsystems interconnections and damping. It is well known that solving PDE's is, in general, not easy. However, the particular PDE that appears in IDA–PBC is parameterized in terms of the desired interconnection and damping matrices, which can be judiciously chosen invoking physical considerations to solve it. This point has been illustrated in several practical applications including mass–balance systems, electrical motors, magnetic levitation systems, power systems, power converters, satellite control and underwater vehicles. See [18] for a list of references.

The present paper, which is an expanded version of [21] and [11], is concerned with the application of IDA–PBC to the problem of stabilization of *underactuated mechanical* systems.[1] Our main contribution is the characterization of a class of systems for which IDA–PBC yields a smooth stabilizing controller. The class is given in terms of solvability of two PDE's that correspond to the potential and kinetic energy shaping stages of the design. As illustrations we design asymptotically stabilizing IDA–PBCs for the well-known ball and beam system and for a novel inverted pendulum. For the ball and beam we prove that for all initial conditions (except a set of zero measure) we drive the beam to the right orientation and define a domain of attraction that ensures that the ball remains within the bar. For the inertia wheel we present a dynamic nonlinear output feedback which, again for "almost" all initial conditions, stabilizes its upward position. That is, we show that it is possible to swing up and balance this pendulum without either switching or measurement of velocities.

Another concern of our paper is to place the new Hamiltonian approach in perspective with the method of "controlled Lagrangians" for stabilization of simple mechanical systems developed

[1]We should point out that, as presented here, IDA–PBC applies only to smoothly stabilizable systems, ruling out the large class considered in [23]. However, the version of IDA–PBC of [9], applies as well to problems involving time–varying Hamiltonians, allowing to consider stabilization with time–varying controllers.

in a series of papers by Bloch et al. (e.g., [5, 6]), and followed up by [1, 3].[2] IDA–PBC and the controlled Lagrangians method are procedures to generate state–feedbacks that transform a given Hamiltonian (respectively, EL) system into another Hamiltonian (respectively, EL) system. A central difference between the methods is that while the target EL dynamics in the controlled Lagrangian method is obtained modifying only the generalized inertia matrix and the potential energy function, in IDA–PBC we have *also* the possibility of changing the interconnection matrix, i.e., the Poisson structure of the system. In this respect, the following questions naturally arise:

1. What is the specific choice of this free parameter that yields the same controllers for both methods? Although the answer to this question has already been reported in our previous papers, e.g., [19], we use here the more recent results of [4] to sharpen the statement.

2. Can we use this additional degree of freedom to simplify the task of solving the aforementioned PDE's? To answer this question we write the PDE's in a form where the free parameters appear explicitly as designer–chosen "control" inputs, and work out two classical examples to illustrate how to select these "inputs".

3. Is the set of *EL* closed–loop models achievable via IDA–PBC "larger" than the one achievable with Lagrangian methods? And if so, can we characterize the gap? We provide here an answer to both questions, showing that with IDA–PBC we can, *still preserving the EL structure*, add gyroscopic terms to the closed–loop system, a feature that is not included in the reported literature with the Lagrangian approach.[3]

To further clarify the connections between IDA–PBC and controlled Lagrangians we—again invoking [4]—prove that the matching conditions of [5] characterize a class of mechanical systems such that its kinetic energy functions can be shaped (to a take a particular form) without solving the aforementioned PDE's. Obviating the need of solving the PDE's, which is the main stumbling block in both approaches, clearly enlarges the applicability of these design methods.

The remaining of the paper is organized as follows. In Section 2 we present the application of IDA–PBC to underactuated mechanical systems. Section 3 is devoted to the comparison between IDA–PBC and the method of controlled Lagrangians. Section 4 summarizes some results available on solvability of the PDE's. Sections 5 and 6 contain the derivations of IDA–PBCs for the inertia wheel pendulum and the ball and beam system, respectively. We wrap up the paper with some concluding remarks in Section 7.

2 Stabilization of Underactuated Mechanical Systems

In this section we apply the IDA-PBC approach to regulate the position of underactuated mechanical systems with total energy

$$H(q,p) = \frac{1}{2} p^\top M^{-1}(q) p + V(q) \tag{2.1}$$

where $q \in I\!R^n$, $p \in I\!R^n$ are the generalized position and momenta, respectively, $M(q) = M^\top(q) > 0$ is the inertia matrix, and $V(q)$ is the potential energy. If we assume that the system has no natural

[2]See [12] for an elegant extension to general Lagrangian systems.

[3]Recently, Bloch et al. [7] have extended the controlled Lagrangian approach to obtain a method equivalent to the IDA-PBC. See Section 3 for more information.

damping, then the equations of motion can be written as[4]

$$\begin{bmatrix} \dot{q} \\ \dot{p} \end{bmatrix} = \begin{bmatrix} 0 & I_n \\ -I_n & 0 \end{bmatrix} \begin{bmatrix} \nabla_q H \\ \nabla_p H \end{bmatrix} + \begin{bmatrix} 0 \\ G(q) \end{bmatrix} u \tag{2.2}$$

The matrix $G \in I\!R^{n \times m}$ is determined by the manner in which the control $u \in I\!R^m$ enters into the system and is invertible in case the system is fully actuated, i.e. $m = n$. We consider here the more difficult case where the system is underactuated, and assume $\text{rank}(G) = m < n$.

In the IDA-PBC method we follow the two basic steps of PBC [20]: 1) *energy shaping*, where we modify the total energy function of the system to assign the desired equilibrium $(q^*, 0)$; and 2) *damping injection* to achieve asymptotic stability. As explained below, to preserve the energy interpretation of the stabilization mechanism we also require the closed–loop system to be in port–controlled Hamiltonian form [28].

2.1 Target Dynamics

Motivated by (2.1) we propose the following form for the desired (closed loop) energy function

$$H_d(q,p) = \frac{1}{2} p^\top M_d^{-1}(q) p + V_d(q) \tag{2.3}$$

where $M_d = M_d^\top > 0$ and V_d represent the (to be defined) closed–loop inertia matrix and potential energy function, respectively. We will require that V_d have an isolated minimum at q_*, that is

$$q_* = \arg\min V_d(q) \tag{2.4}$$

In PBC the control input is naturally decomposed into two terms

$$u = u_{es}(q,p) + u_{di}(q,p) \tag{2.5}$$

where the first term is designed to achieve the energy shaping and the second one injects the damping. The desired port–controlled Hamiltonian dynamics are taken of the form[5]

$$\begin{bmatrix} \dot{q} \\ \dot{p} \end{bmatrix} = [J_d(q,p) - R_d(q,p)] \begin{bmatrix} \nabla_q H_d \\ \nabla_p H_d \end{bmatrix} \tag{2.6}$$

where the terms

$$J_d = -J_d^\top = \begin{bmatrix} 0 & M^{-1} M_d \\ -M_d M^{-1} & J_2(q,p) \end{bmatrix} \; ; \; R_d = R_d^\top = \begin{bmatrix} 0 & 0 \\ 0 & G K_v G^\top \end{bmatrix} \geq 0$$

represent the desired interconnection and damping structures.

The following observations are in order:

- From (2.1), (2.2) we have that $\dot{q} = M^{-1} p$. Since this is a non–actuated coordinate this relationship should hold also in closed–loop. Fixing (2.3) and (2.6) determines the $(1,2)$–block of J_d.

[4]Throughout the paper we view all vectors, including the gradient, as column vectors; except in the Hessian matrix where they appear as rows.

[5]See [18, 28] for the physical and analytical justification of this choice.

– The matrix R_d is included to add damping into the system. As is well–known, this is achieved via negative feedback of the (new) passive output (also called L_gV control), which in this case is $G^\top \nabla_p H_d$. That is, we will select the second term of (2.5) as

$$u_{di} = -K_v G^\top \nabla_p H_d \tag{2.7}$$

where we take $K_v = K_v^\top > 0$. This explains the $(2,2)$–block of R_d.

– We will show below that the skew–symmetric matrix J_2 (and some of the elements of M_d) can be used as *free parameters* in order to achieve the kinetic energy shaping. Providing these degrees of freedom is the essence of IDA–PBC.[6]

2.2 Stability

For the desired closed–loop dynamics we have the following proposition, which reveals the stabilization properties of our approach:

Proposition 1 *The system (2.6), with (2.3) and (2.4), has a stable equilibrium point at $(q_*, 0)$. This equilibrium is asymptotically stable if it is locally detectable from the output*[7] $G^\top(q)\nabla_p H_d(q,p)$. *An estimate of the domain of attraction is given by $\Omega_{\bar{c}}$ where $\Omega_c \stackrel{\triangle}{=} \{(q,p) \in I\!R^{2n} \mid H_d(q,p) < c\}$ and*

$$\bar{c} \stackrel{\triangle}{=} \sup\{c > H_d(q_*, 0) \mid \Omega_c \text{ is bounded}\} \tag{2.8}$$

Proof. From (2.3) and (2.4) we have that H_d is a positive definite function in a neighborhood of $(q_*, 0)$. A straightforward calculation shows that, along trajectories of (2.6), $\dot{H}_d$ satisfies

$$\begin{aligned} \dot{H}_d &= (\nabla_q H_d)^\top \dot{q} + (\nabla_p H_d)^\top \dot{p} \\ &= -(\nabla_p H_d)^\top G K_v G^\top \nabla_p H_d \\ &\leq -\lambda_{min}\{K_v\} |(\nabla_p H_d)^\top G|^2 \leq 0 \end{aligned}$$

since J_d is skew–symmetric and K_v is positive definite. Hence, $(q_*, 0)$ is a stable equilibrium. Furthermore, since (by definition) H_d is proper on its sub–level set $\Omega_{\bar{c}}$, all trajectories starting in $\Omega_{\bar{c}}$ are bounded. Asymptotic stability, under the detectability assumption, is established invoking Barbashin–Krasovskii's theorem and the arguments used in the proof of Theorem 3.2 of [8]. Finally, the estimate of the domain of attraction follows from the fact that $\Omega_{\bar{c}}$ is the largest bounded sub–level set of H_d. ◁

2.3 Energy Shaping

To obtain the energy shaping term, u_{es}, of the controller we replace (2.5) and (2.7) in (2.2) and equate it with (2.6)[8]

$$\begin{bmatrix} 0 & I_n \\ -I_n & 0 \end{bmatrix} \begin{bmatrix} \nabla_q H \\ \nabla_p H \end{bmatrix} + \begin{bmatrix} 0 \\ G \end{bmatrix} u_{es} = \begin{bmatrix} 0 & M^{-1} M_d \\ -M_d M^{-1} & J_2(q,p) \end{bmatrix} \begin{bmatrix} \nabla_q H_d \\ \nabla_p H_d \end{bmatrix}$$

[6] In Section 3 we will show that, for a *particular choice* of skew–symmetric J_2, IDA–PBC reduces to the controlled Lagrangian schemes of [1, 12, 6]. It is reasonable to expect that the possibility of choosing among the whole class of skew–symmetric matrices enlarges the class of stabilizable systems.

[7] That is, for any solution $(q(t), p(t))$ of the closed–loop system which belongs to some open neighborhood of the equilibrium for all $t \geq 0$, the following implication is true:

$$G^\top(q(t))\nabla_p H_d(q(t), p(t)) \equiv 0, \forall t \geq 0 \Rightarrow \lim_{t \to \infty} (q(t), p(t)) = (q_*, 0).$$

[8] Notice that the damping matrix cancels with u_{di}.

While the first row of equations above is clearly satisfied, the second set of equations can be expressed as

$$Gu_{es} = \nabla_q H - M_d M^{-1} \nabla_q H_d + J_2 M_d^{-1} p$$

Now, it is clear that if G is invertible, i.e., if the system is fully actuated, then we may uniquely solve for the control input u_{es} given any H_d and J_2. In the underactuated case, G is not invertible but only full column rank, and u_{es} can only influence the terms in the range space of G. This leads to the following set of constraint equations, which must be satisfied for any choice of u_{es},

$$G^{\perp}\{\nabla_q H - M_d M^{-1} \nabla_q H_d + J_2 M_d^{-1} p\} = 0 \tag{2.9}$$

where $G^{\perp}$ is a full rank left annihilator of G, i.e., $G^{\perp}G = 0$. Equation (2.9), with H_d given by (2.3), is a set of nonlinear PDE's with unknowns M_d and V_d, with J_2 a *free* parameter, and p an independent coordinate. If a solution for this PDE is obtained, the resulting control law u_{es} is given as

$$u_{es} = (G^{\top}G)^{-1}G^{\top}(\nabla_q H - M_d M^{-1} \nabla_q H_d + J_2 M_d^{-1} p) \tag{2.10}$$

The PDE's (2.9) can be naturally separated into the terms that depend on p and terms which are independent of p, i.e., those corresponding to the kinetic and the potential energies, respectively. Thus, (2.9) can be equivalently written as

$$G^{\perp}\left\{\nabla_q(p^{\top}M^{-1}p) - M_d M^{-1}\nabla_q(p^{\top}M_d^{-1}p) + 2J_2 M_d^{-1}p\right\} = 0 \tag{2.11}$$

$$G^{\perp}\{\nabla_q V - M_d M^{-1}\nabla_q V_d\} = 0 \tag{2.12}$$

The first equation is a nonlinear PDE that has to be solved for the unknown elements of the closed–loop inertia matrix M_d. Given M_d, equation (2.12) is a simple linear PDE, hence the main difficulty is in the solution of (2.11). Equation (2.11) can be expressed in a more explicit form with the following derivations. First, we use the fact that $\nabla_q(z^{\top}P(q)z) = [\nabla_q(P(q)z)]^{\top}z$, for all $z \in I\!R^n$ and all symmetric $P \in I\!R^{n\times n}$, to write (2.11) as

$$G^{\perp}\left\{\left[[\nabla_q(M^{-1}p)]^{\top} - M_d M^{-1}[\nabla_q(M_d^{-1}p)]^{\top} + 2J_2 M_d^{-1}\right]p\right\} = 0$$

Then, we apply the identity

$$\nabla_q(P(q)z) = \sum_{k=1}^{n} \nabla_q(P_{(\cdot,k)})z_k$$

which holds for all $z \in I\!R^n$ and all $P \in I\!R^{n\times n}$, where $P_{(\cdot,k)}$ denotes the k–th column of the matrix P, reparametrize J_2 in terms of the matrices $U_k(q) = -U_k^{\top}(q) \in I\!R^{n\times n}$ as

$$2J_2 = \sum_{k=1}^{n} U_k p_k \tag{2.13}$$

and equate terms in p_k to obtain n PDE's, expressed only in terms of the independent variable q, of the form

$$G^{\perp}\left\{\left[\nabla_q(M^{-1}_{(\cdot,k)})\right]^{\top} - M_d M^{-1}\left[\nabla_q(M_d^{-1})_{(\cdot,k)}\right]^{\top} + U_k M_d^{-1}\right\} = 0 \tag{2.14}$$

where U_k are *designer chosen* matrices.

The key idea is then to chose the free parameters U_k in such a way that (2.14) admits a solution with M_d symmetric and positive definite. Then, we replace it into (2.12), which is a linear PDE, and look for a solution V_d which satisfies (2.4). The additional degree of freedom provided by U_k is the main feature that distinguishes IDA–PBC from the Lagrangian methods that we review in the next section.

The following remarks are in order

- The derivations above characterize a class of underactuated mechanical systems for which the newly developed IDA–PBC design methodology yields smooth stabilization. The class is given in terms of solvability of the nonlinear PDE (2.11), (or the more explicit (2.14)), and the linear PDE (2.12). Although it is well–known that solving PDE's is in general hard, it is our contention that the added degree of freedom—the closed–loop interconnection J_2 (equivalently, U_k)—simplifies this task. We will elaborate further on this point in Section 3 and in the examples below.

- There are two "extreme" particular cases of our procedure. First, if we do not modify the interconnection matrix then we recover the well–known potential energy shaping procedure of PBC. Indeed, if $M_d = M$ and $J_2 = 0$, then the controller equation (2.10) reduces to

$$u_{es} = (G^\top G)^{-1} G^\top (\nabla_q V - \nabla_q V_d)$$

  which is the familiar potential energy shaping control. On the other extreme, if we do not change the potential energy, but only modify the kinetic energy then, as we will show in the next section, for a particular choice of J_2, i.e., (3.6), we recover the controlled–Lagrangian method of [5]. Now, if we shape both kinetic and potential energies, but fix J_2 to (3.6), then IDA–PBC coincides with the method proposed in [1, 13].

3 Comparison with the Lagrangian Approach

The IDA–PBC method may be interpreted as a procedure to generate state–feedback controllers that transform a given port–controlled Hamiltonian system into another port–controlled Hamiltonian system with some desired stability properties, e.g., in the case of mechanical systems to transform (2.1), (2.2) into (2.3), (2.6) for some positive definite inertia matrix M_d, a potential function V_d satisfying (2.4), and an arbitrary skew–symmetric matrix J_2. Viewed from this perspective, the PDE's (2.11) and (2.12) constitute some matching conditions (that ensure that the solutions $(q(t), p(t))$ of both systems are the same.) A similar approach can be taken proceeding from a Lagrangian perspective. That is, starting from an EL system

$$\frac{d}{dt}\nabla_{\dot q} L(q,\dot q) - \nabla_q L(q,\dot q) = G(q)u$$

where L is the Lagrangian, defined as the *difference* between the kinetic and the potential energies, we want to find a static state feedback such that the behavior of the closed–loop is described by the controlled Lagrangian system

$$\frac{d}{dt}\nabla_{\dot q} L_c(q,\dot q) - \nabla_q L_c(q,\dot q) = 0 \tag{3.1}$$

where L_c is the desired Lagrangian. This problem has been studied in great generality in [12], see also [4]. For the case of interest here, that is, restricted to Lagrangians of the form

$$L = \frac{1}{2}\dot q^\top M(q)\dot q - V(q), \qquad L_c = \frac{1}{2}\dot q^\top M_c(q)\dot q - V_c(q), \tag{3.2}$$

it has been shown in [1, 13] that the set of achievable Lagrangians L_c is characterized by the solvability of the PDE's[9]

$$G^{\perp}\left\{[\nabla_q(M\dot{q}) - MM_c^{-1}\nabla_q(M_c\dot{q})]\dot{q} - \frac{1}{2}\left[\nabla_q(\dot{q}^\top M\dot{q}) - MM_c^{-1}\nabla_q(\dot{q}^\top M_c\dot{q})\right]\right\} = 0 \quad (3.3)$$

$$G^{\perp}\{\nabla_q V - MM_c^{-1}\nabla_q V_c\} = 0 \quad (3.4)$$

which, similarly to (2.11), (2.12) of IDA–PBC, match the kinetic and the potential energy terms.[10] Recalling that $p = M\dot{q}$ and defining a matrix

$$M_c(q) \triangleq MM_d^{-1}M \quad (3.5)$$

which is clearly symmetric and positive definite, we see that (3.4) exactly coincides with (2.12)—setting $V_c = V_d$. Furthermore, equation (2.11) *reduces* to (3.3) if and only if

$$J_2(q,p) = M_d M^{-1}\left\{[\nabla_q(MM_d^{-1}p)]^\top - \nabla_q(MM_d^{-1}p)\right\} M^{-1}M_d \quad (3.6)$$

Although the expression above can be verified via direct substitution, a more elegant proof is given in [4] checking that the (energy conserving part of the) port–controlled Hamiltonian system (2.3), (2.6) is equivalent to the EL (mechanical) system

$$\begin{bmatrix} \dot{q} \\ \dot{p}_c \end{bmatrix} = \begin{bmatrix} 0 & I_n \\ -I_n & 0 \end{bmatrix} \begin{bmatrix} \nabla_q H_c \\ \nabla_{p_c} H_c \end{bmatrix}$$

where $p_c = M_c\dot{q}$ and $H_c(q,p_c) = \frac{1}{2}p_c^\top M_c^{-1}(q)p_c + V_c(q)$. An alternative form for J_2 can be obtained as

$$(J_2)_{(i,j)} = -p^\top M_d^{-1}M\left[(M^{-1}M_d)_{(\cdot,i)}, (M^{-1}M_d)_{(\cdot,j)}\right]$$

with $[\cdot,\cdot]$ the standard Lie bracket and $(\cdot)_{(i,j)}$ denotes the (i,j) term of a matrix. (This expression was first reported in [19], although with swapped sub-indices due to an unfortunate typo.)

It has also been shown in [4] that we can add to (3.6) a (skew-symmetric) matrix of the form $M_d M^{-1}\{[\nabla_q Q(q)]^\top - \nabla_q Q(q)\}M^{-1}M_d$, with Q an arbitrary function of q, still preserving the closed loop EL structure (3.1). This corresponds to the closed–loop Lagrangian

$$L_c = \frac{1}{2}\dot{q}^\top M_c\dot{q} + \dot{q}^\top Q - V_c$$

that includes the gyroscopic terms $\dot{q}^\top Q$, which are proven to be *intrinsic*—roughly speaking, this means that they cannot be removed with a change of coordinates. In other words, IDA-PBC naturally generates a 'richer' class of matchable EL systems of the form (3.1), which have not been considered in the literature of the Lagrangian approach.

Recently Bloch et al. [7] have shown that a small adjustment in the controlled Lagrangian approach yields a method which is fully equivalent with IDA-PBC as described in this paper. Essentially, instead of restricting to systems of the form (3.1), they also allow to include some external forces into the closed-loop Euler-Lagrange system (i.e., the right hand side of (3.1) is not necessarily equal to zero, but can be any external force). In this way, it is possible to write any mechanical Hamiltonian system in Euler-Lagrange format by including the non-integrable part of the Hamiltonian system as an external (gyroscopic) force into the Euler-Lagrange system. Notice that this method only works for the class of simple mechanical systems, as presented in this paper. Considering this larger class of closed-loop EL systems [7] establishes that the controlled Lagrangian method is *equivalent* to the IDA-PBC method.

[9] In the cited references the PDE (3.3) is expressed using the Christoffel symbols of the second kind, which leads to a more elegant and compact notation. To avoid introducing additional notation we prefer to use the form given here.

[10] In [17], see also [18], we derive matching conditions—expressed in terms of algebraic constraints—for *potential* energy shaping of EL systems in closed–loop with *dynamic* EL controllers.

4 Methods for Solving the Matching PDE's

Our derivations above showed that in both approaches, Lagrangian or Hamiltonian, it is necessary to solve some PDE's—a task that is, in general, difficult. We recall now some results reported in the literature that allows us to simplify this problem.

First, it has been shown in [10] that if $m = n - 1$ (i.e., the system is underactuated only by one degree of freedom), and the kinetic energy matrix M depends only on the unactuated coordinate, then the nonlinear PDE (2.11) can be transformed, with a suitable choice of M_d and J_2, into a set of *ordinary differential equations* (ODE's), hence easier to solve. More precisely, if we let k be the index of the non–actuated coordinate, and assume that

$$\begin{aligned} G^{\perp} &= e_k^{\top} \\ \nabla_q M_{(i,j)} &= \frac{dM_{(i,j)}}{dq_k} e_k \end{aligned}$$

Then, restricting M_d to be only a function of q_k, it is possible to show that (2.11) reduces to the ODE's

$$\frac{d}{dq_k}(M_d)_{(\cdot,k)} = -\frac{1}{(M_d M^{-1})_{(k,k)}} \left(M_d \frac{d}{dq_k}(M^{-1}) M_d \right)_{(\cdot,k)} \tag{4.1}$$

The class of systems that satisfies these assumptions is quite common in the control literature including the two examples considered here, namely, the inertia wheel pendulum and the classical ball and beam, as well as the cart and pendulum which is studied in [10]. For the first example the inertia matrix M is constant and we can take M_d also independent of q and $J_2 = 0$, obviating the solution of (2.11). On the other hand, we will show later that for the second example the reduction to ordinary differential equations is instrumental to solve the problems.

Second, we have shown in Section 3 that if we fix J_2 as (3.6), which ensures that the closed–loop system admits an EL representation of the form (3.1), (3.2), then the nonlinear PDE (2.11) reduces to (3.3). An important contribution of [1], see also [3], [2], is the proof that all of the solutions of these PDE's may be obtained by sequentially solving a set of three first order *linear* PDE's. It has been show in [4] that the techniques used in [1] can be extended to the study of the PDE (2.11), which incorporate the free parameter U_k. In fact, this leads to a set of one quadratic and two linear first order PDEs. The first PDE is quadratic in the sense that it contains terms quadratic in the to–be–solved-variables, the derivatives however still appear linearly in the equation.

Third, in a series of interesting papers, e.g., [5, 6], Bloch et al. have proven that, in some cases which includes some well–known examples, the solution of these PDE's can actually be *obviated.* In [4] we have interpreted these conditions using the notation employed in this paper. We now briefly summarize these results. Towards this end, we find it convenient to partition the generalized coordinates as $q = [x^{\top}, \theta^{\top}]^{\top}$, with $x \in I\!R^r$, $\theta \in I\!R^{n-r}$. This induces a natural partition of the open–loop inertia matrix as

$$M = \begin{bmatrix} M^{xx} & M^{x\theta} \\ M^{\theta x} & M^{\theta\theta} \end{bmatrix}$$

As in [5], we now introduce the following assumptions:

(i) The Lagrangian is independent of the θ coordinates, i.e., they are *cyclic* variables. In this case the Lagrangian takes the form $L(x, \dot{q}) = \frac{1}{2}\dot{q}^{\top} M(x)\dot{q} - V(x)$.

(ii) The θ–coordinates are fully actuated, that is $G = [0 \;\; I]^{\top}$.

(iii) The matrix M has the block $M^{\theta\theta}$ *constant*, and satisfies[11]

$$\nabla_{x_j} M^{x_i\theta_k} = \nabla_{x_i} M^{x_j\theta_k}, \;\; i,j = 1,\ldots,r; \; k = 1,\ldots,n-r$$

Now, let us take the controlled Lagrangian as $L_c(x,\dot{q}) = \frac{1}{2}\dot{q}^\top M_c(x)\dot{q} - V(x)$. (Notice that, as in [5], we only aim at kinetic energy shaping.) A first immediate observation is that in this case, under the assumptions (i), (ii), the matching condition (3.4) reduces to an *algebraic* equation

$$[I \;\; 0](I - MM_c^{-1})\begin{bmatrix} I \\ 0 \end{bmatrix} \nabla_x V = 0 \tag{4.2}$$

A central contribution of [5] is the proof that, for the following particular class of M_c, satisfying the so–called, simplified matching assumptions,

$$M_c = M + \begin{bmatrix} \kappa(\kappa+1)M^{x\theta}(M^{\theta\theta})^{-1}M^{\theta x} & \kappa M^{x\theta} \\ \kappa M^{\theta x} & 0 \end{bmatrix},$$

with $\kappa \in I\!R$, the PDE's (3.4), (3.3) are automatically satisfied.

In [4] we have shown that, for the class of M_c considered in [5], their first matching condition M-1 is equivalent to the algebraic condition

$$[I \;\; 0](I - MM_c^{-1})\begin{bmatrix} I \\ 0 \end{bmatrix} = 0,$$

which in the light of (4.2), clearly obviates the potential energy PDE (3.4). Furthermore, it is also established that the matching conditions M-2 and M-3 of [5] exactly coincide with the PDE (3.3).

We should recall that solving the PDE's (3.3), (3.4) is just the first step in the design procedure. Indeed, to establish stability using Proposition 1 the matrix M_d should be positive definite (at least in a neighborhood of the equilibrium q_*), further, V_d should have an isolated local minimum in q_*. In Theorem 3.4 of [5] it has been shown that relative equilibria, i.e., equilibria of the form $(x = \bar{x}, \dot{x} = 0, \dot{\theta} = 0)$, of *conservative* systems are stable if the Hessian of the total energy is *definite* (either positive or negative). Although hard to justify from a physical viewpoint, we can in this way use these methods to locally stabilize (relative equilibria of) conservative mechanical systems with a *negative definite* closed–loop inertia matrix. This feature is essential in [5] where the potential energy is not modified by the control, and will typically have a maximum at the desired equilibrium, hence the kinetic energy should also have a maximum at this point. The qualifier "conservative" is also important because it is not clear to these authors how to handle the presence of physical damping in this framework.

5 The Inertia Wheel Pendulum

In this section we apply the preceding design methodology to the problem of stabilizing the inverted position of the inertia wheel pendulum shown in Fig. 1, which consists of a physical pendulum with a balanced rotor at the end. The motor torque produces an angular acceleration of the end-mass which generates a coupling torque at the pendulum axis. We show that the IDA-PBC provides an affirmative answer to the question of existence of a *continuous* control law that, for all initial conditions except a set of zero measure, swings up and balances in the upward position the pendulum.[12] We also show that, as usual in PBC [18], the passivity property allows us to replace the state-feedback control by a dynamic *output* feedback that does not require the measurements of velocities.

[11] These are the simplified matching assumptions 2 and 4 of [5], respectively.

[12] This means that the basin of attraction of our controller is an open dense set in the state space, which is the best one can hope for using a continuous feedback [26].

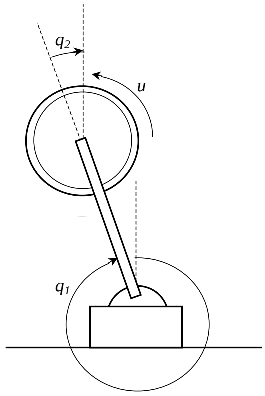

Figure 1: Inertia Wheel Pendulum.

5.1 Model

The dynamic equations of the device can be written in standard form using the EL formulation [27] as

$$\begin{bmatrix} I_1 + I_2 & I_2 \\ I_2 & I_2 \end{bmatrix} \begin{bmatrix} \ddot{\theta}_1 \\ \ddot{\theta}_2 \end{bmatrix} + \begin{bmatrix} -mgL\sin(\theta_1) \\ 0 \end{bmatrix} = \begin{bmatrix} 0 \\ 1 \end{bmatrix} u$$

where θ_1, θ_2 and I_1, I_2 are the respective angles and moments of inertia of the pendulum and disk, m is the pendulum mass, L its length, g the gravity constant, and u is the control input torque acting between the disk and pendulum. The change of coordinates

$$\begin{bmatrix} q_1 \\ q_2 \end{bmatrix} = \begin{bmatrix} \theta_1 \\ \theta_1 + \theta_2 \end{bmatrix}$$

leads to the simplified description

$$\begin{bmatrix} I_1 & 0 \\ 0 & I_2 \end{bmatrix} \begin{bmatrix} \ddot{q}_1 \\ \ddot{q}_2 \end{bmatrix} + \begin{bmatrix} -m_3\sin(q_1) \\ 0 \end{bmatrix} = \begin{bmatrix} -1 \\ 1 \end{bmatrix} u \tag{5.1}$$

where $m_3 \stackrel{\triangle}{=} mgL$. The system can be written in Hamiltonian form (2.2) with $p = [I_1\dot{q}_1, I_2\dot{q}_2]^\top$, the total energy function (2.1) and

$$M = \begin{bmatrix} I_1 & 0 \\ 0 & I_2 \end{bmatrix}, \qquad G = \begin{bmatrix} -1 \\ 1 \end{bmatrix}, \qquad V(q_1) = m_3(\cos q_1 - 1)$$

The equilibrium to be stabilized is the upward position with the inertia disk aligned, which corresponds to $q_1^* = q_2^* = 0$.[13]

Caveat The model of the inertia wheel pendulum can be seen either as a system defined over $\mathbb{R}^4$ or, taking q_1 modulo 2π, over $\mathcal{S} \times \mathbb{R}^3$, with $\mathcal{S}$ the unit circle. To allow for feedback laws that are not necessarily 2π–periodic on q_1 we adopt the former one for the controller design. However, to determine the domain of attraction we look at the system in the cylinder.

[13] Since the mass distribution of the inertia disk is symmetric, it may be argued that there is no particular reason for aligning it. In spite of that, we impose this objective to illustrate the generality of the approach.

5.2 Controller Design

We will design our IDA-PBC in three steps. First, we will obtain a state-feedback that shapes the energy to globally stabilize the upward position, then we add the damping for asymptotic stability by feedback of the passive output. Finally, we show that it is possible to replace the velocity feedback by its dirty derivative preserving asymptotic stability.

A. Energy Shaping

First, notice that the inertia matrix M is independent of q, hence, we can take $J_2 = 0$ and M_d to be a *constant* matrix too, which we denote by

$$M_d = \begin{bmatrix} a_1 & a_2 \\ a_2 & a_3 \end{bmatrix}$$
$$a_1 > 0,\ a_1 a_3 > a_2^2 \tag{5.2}$$

The inequalities for the coefficients are imposed to ensure M_d is positive definite. The only PDE to be solved is then the potential energy PDE given by Equation (2.12), that is

$$\left(\frac{a_1 + a_2}{I_1}\right)\frac{\partial V_d}{\partial q_1} + \left(\frac{a_2 + a_3}{I_2}\right)\frac{\partial V_d}{\partial q_2} = -m_3 \sin(q_1)$$

This is a trivial linear PDE whose general solution is of the form

$$V_d(q) = \frac{I_1 m_3}{a_1 + a_2}\cos(q_1) + \Phi\left(z(q)\right) \tag{5.3}$$
$$z(q) = q_2 + \gamma_2 q_1 \tag{5.4}$$

where Φ is an arbitrary differentiable function that we must choose to satisfy the condition (2.4) for $q_* = 0$. We have also defined $\gamma_2 \triangleq -I_1(a_2 + a_3)/(I_2(a_1 + a_2))$. Some simple calculations show that the necessary condition $\nabla_q V_d(0) = 0$ is satisfied if and only if $\nabla\Phi(z(0)) = 0$, while the sufficient condition $\nabla_q^2 V_d(0) > 0$ will hold if the Hessian of Φ at the origin is positive, and

$$a_2 < -a_1 \tag{5.5}$$

These conditions on Φ are satisfied with the choice[14] $\Phi(z) = \frac{k_1}{2}z^2$, where $k_1 > 0$ represents an adjustable gain.

The energy shaping term of the control input (2.10) is given as

$$\begin{aligned} u_{es} &= (G^\top G)^{-1}G^\top(\nabla_q V - M_d M^{-1}\nabla_q V_d) \\ &= \frac{1}{2}\left[\left(\frac{a_1 - a_2}{I_1}\right)\frac{\partial V_d}{\partial q_1} + \left(\frac{a_2 - a_3}{I_2}\right)\frac{\partial V_d}{\partial q_2} + m_3 \sin(q_1)\right] \\ &= \gamma_1 \sin(q_1) + k_p(q_2 + \gamma_2 q_1) \end{aligned} \tag{5.6}$$

where we have defined

$$\gamma_1 \triangleq \frac{a_2}{a_1 + a_2} m_3 \qquad k_p \triangleq -k_1\left[\frac{a_1 a_3 - a_2^2}{I_2(a_1 + a_2)}\right]$$

We recall that a_1, a_2, a_3 should satisfy the inequalities (5.2) and (5.5), some simple calculations show that these conditions translate into

$$\gamma_1 > m_3 \qquad \gamma_2 > \frac{I_1}{I_2}\frac{\gamma_1}{\gamma_1 - m_3} \tag{5.7}$$

which, together with $k_p > 0$, define the *admissible region* for the tuning gains.

[14]For simplicity we have taken here a quadratic function Φ. Clearly other options, that may be selected to improve the transient performance, are possible; e.g., a saturated function.

B. Damping Injection and Stability Analysis

The control law $u = u_{es} + u_{di}$ results in the system

$$\begin{bmatrix} \dot{q} \\ \dot{p} \end{bmatrix} = \begin{bmatrix} 0 & M^{-1}M_d \\ -M_d M^{-1} & 0 \end{bmatrix} \begin{bmatrix} \nabla_q H_d \\ \nabla_p H_d \end{bmatrix} + \begin{bmatrix} 0 \\ G \end{bmatrix} u_{di}$$

for which we have $\dot{H}_d = \nabla_p H_d{}^\top G u_{di}$. Clearly, without damping injection the origin is a stable equilibrium. To make this equilibrium *asymptotically* stable we propose to add damping feeding back the new passive output $\nabla_p H_d{}^\top G$, which can be computed as

$$\begin{aligned} G^\top \nabla_p H_d &= \frac{1}{a_1 a_3 - a_2^2}\left[-(a_2+a_3)p_1 + (a_1+a_2)p_2\right] \\ &= k_2(\dot{q}_2 + \gamma_2 \dot{q}_1) \end{aligned} \tag{5.8}$$

where we defined $k_2 \triangleq -\frac{I_2(a_1+a_2)}{a_1 a_3 - a_2^2} > 0$, with positivity following from (5.2) and (5.5).

We are in position to present our first stabilization result, which establishes that for all initial conditions—except a set of zero measure—the IDA–PBC drives the pendulum to its upward position with the disk aligned.

Proposition 2 *The inertia wheel pendulum (5.1) in closed-loop with the static state–feedback IDA–PBC*

$$u = \gamma_1 \sin(q_1) + k_p(q_2 + \gamma_2 q_1) - k_v(\dot{q}_2 + \gamma_2 \dot{q}_1) \tag{5.9}$$

where γ_1, γ_2 satisfy (5.7), $k_p > 0$ is a proportional gain, and $k_v > 0$ is a damping injection gain, has an asymptotically stable equilibrium at zero, with domain of attraction the whole state space minus a set of Lebesgue measure zero.

Proof. We first observe that the closed–loop system has equilibria $(\bar{q}, 0)$, where $\bar{q} = (j\pi, k\pi), j, k \in \mathbb{N}$, are the solutions of $\nabla_q V_d(\bar{q}) = 0$. We recall from Fig. 1 that the points $\bar{q}_1$ with k even correspond to the desired upward position, while the ones with odd k are with the pendulum hanging

From Proposition 1 and the derivations above we know that the equilibria corresponding to the upward position of the pendulum are stable. Further, with some basic signal chasing, it is possible to show that—in a neighborhood of zero—the trajectories of the closed–loop system satisfy the (stronger) observability condition: $\dot{H}_d \equiv 0 \Rightarrow (q(t), p(t)) \equiv 0$. Therefore, Proposition 1 insures that the desired equilibrium is asymptotically stable. Although Proposition 1 provides also an estimate of its domain of attraction, we will show below that asymptotic stability is "almost" global—in the sense of Proposition 2.

Towards this end, we make the important observation that the introduction in the control (5.9) of a non–periodic function of q_1 forces us to consider the system in $\mathbb{R}^4$ instead of $\mathcal{S} \times \mathbb{R}^3$, and then H_d is not a proper function of (q, p) and we cannot insure boundedness of trajectories (starting outside $\Omega_{\bar{c}}$.) Nevertheless, in the coordinates $(q_1, \tilde{q}_2, p_1, p_2)$, with $\tilde{q}_2 = q_2 + \gamma_2 q_1$, the closed–loop system is indeed defined over $\mathcal{S} \times \mathbb{R}^3$, and the energy function

$$\tilde{H}_d(q_1, \tilde{q}_2, p_1, p_2) = \frac{1}{2} p^\top M_d^{-1} p + \frac{I_1 m_3}{a_1 + a_2}[\cos(q_1) - 1] + \frac{k_1}{2}\tilde{q}_2^2$$

is positive definite and proper throughout $\mathcal{S} \times \mathbb{R}^3$. Then, since $\dot{\tilde{H}}_d = -k_v k_2 \tilde{q}_2^2 \le 0$, we have that *all solutions* are bounded in $\mathcal{S} \times \mathbb{R}^3$. From the analysis above we know that the zero equilibrium is asymptotically stable. We will now show that the other equilibria are unstable. Indeed, the linearization of the closed–loop system at these equilibria has eigenvalues with strictly positive real part and at least one eigenvalue with strictly negative real part. Associated to the latter there is a stable manifold, and trajectories starting in this manifold will converge to the downward position. However, it is well–known that an s–dimensional invariant manifold of an n–dimensional system has Lebesgue measure zero if $s < n$; see, e.g., [29]. Consequently, the set of initial conditions that converges to the "bad" equilibrium has zero measure.

To complete the proof we establish now that trajectories are also bounded in $I\!R^4$.[15] For, we see that our derivations above have proven that, in $\mathcal{S} \times I\!R^3$, all trajectories are bounded and tend to one of the equilibria $(0,0,0,0)$ or $(\pi,0,0,0)$. The first equilibrium is asymptotically stable and the second one is hyperbolic. We have furthermore shown that almost any solution converges to the stable equilibrium, being trapped in finite time in a sufficiently small neighborhood of it, say $\mathcal{N}_0$. Let us now immerse the cylinder in the Euclidean space $I\!R^4$, and consider the sets of $I\!R^4$ which correspond to $\mathcal{N}_0$ on the cylinder. If $\mathcal{N}_0$ is chosen sufficiently small, then these sets in $I\!R^4$ do not intersect. Since the solutions on the cylinder do not leave $\mathcal{N}_0$ the immersion of the trajectories will not leave the corresponding neighborhood in $I\!R^4$. This completes the proof. $\triangleleft$

C. Output Feedback

It is well known that in PBC designs it is sometimes possible to obviate velocity measurement feeding back instead the dirty derivative of positions [15]. This feature stems from the fact that for feedback interconnection of passive maps we can replace a *constant* feedback by a feedback through any positive real transfer function preserving stability. In particular, to implement the damping injection we can use the feedback

$$u_{di} = -\frac{k_v D}{\tau D + 1}(q_2 + \gamma_2 q_1)$$

with $D \triangleq \frac{d}{dt}$, and $k_v, \tau > 0$ some filter parameters. The important point is that u_{di} is implementable without velocity feedback. This consideration leads us to our final result contained in the proposition below. The proof follows along the lines of the previous proposition, and is only outlined for brevity.

Proposition 3 *Consider the inertia wheel pendulum (5.1) in closed-loop with the dynamic output feedback IDA–PBC*

$$u = -\gamma_1 \sin(q_1) + k_p(q_2 + \gamma_2 q_1) + u_{di}$$

where γ_1, γ_2 satisfy (5.7), $k_p > 0$ is a proportional gain; u_{di} is a damping injection term generated from the dirty derivative of the positions as

$$\begin{aligned} \dot{\vartheta} &= -\frac{1}{\tau}\vartheta + \frac{k_v}{\tau^2}(q_2 + \gamma_2 q_1) \\ u_{di} &= \vartheta - \frac{k_v}{\tau}(q_2 + \gamma_2 q_1) \end{aligned} \tag{5.10}$$

with $\tau, k_v > 0$. Then, for all initial conditions—except a set of zero measure—the pendulum converges to its upward position with all internal signals uniformly bounded.

Proof. First, notice that from (5.8) and (5.10) we get

$$\dot{u}_{di} = -\frac{1}{\tau}u_{di} - \frac{k_v}{k_2 \tau} G^\top \nabla_p H_d$$

[15] We thank anonymous Reviewer No. 5 for this proof of global boundedness.

Consequently, if we define the new energy function $W(q,p,u_{di}) \triangleq H_d + \frac{k_2\tau}{2k_v}u_{di}^2$, we can write the closed–loop system in port–controlled Hamiltonian form as

$$\begin{bmatrix} \dot{q} \\ \dot{p} \\ \dot{u}_{di} \end{bmatrix} = \begin{bmatrix} \begin{bmatrix} 0 & M^{-1}M_d \\ -M_dM^{-1} & 0 \end{bmatrix} & \begin{bmatrix} 0 \\ \frac{k_v}{k_2\tau}G \end{bmatrix} \\ \begin{bmatrix} 0 & -\frac{k_v}{k_2\tau}G^\top \end{bmatrix} & -\frac{k_v}{k_2\tau^2} \end{bmatrix} \begin{bmatrix} \nabla_q W \\ \nabla_p W \\ \nabla_{u_{di}} W \end{bmatrix}$$

We have $\dot{W} = -\frac{k_2}{k_v}(u_{di})^2$. The proof is completed proceeding as in Proposition 2. $\triangleleft$

5.3 Simulation Results

We simulated the response of the inertia wheel pendulum using the system parameters $I_1 = .1, I_2 = .2, m_3 = 10$ and the full state feedback controller with tuning gains $\gamma_1 = 30,\ \gamma_2 = 0.2$. The following plots show the response of the system starting at rest with initial configuration $q(0) = (3,0)$. Thus the pendulum is hanging nearly vertically downward.

In order to illustrate the influence of the choice of k_p and k_v on the transient behavior, we have put together several plots of $q_1(t)$ and $q_2(t)$, first only changing k_p with k_v kept constant at a value of 10 as seen in Fig. 2. A simple observation shows that larger values of k_p slow down the convergence towards the equilibrium point. Leaving k_p constant and changing k_v from 10 to 100, the plots in Fig. 3 are obtained. These plots show that, counter intuitively but not totally unexpected, the oscillations vanish faster for lower values of k_v! Finally, Fig. 4 shows the applied control torque when $k_p = 0.1$ and $k_v = 10$.

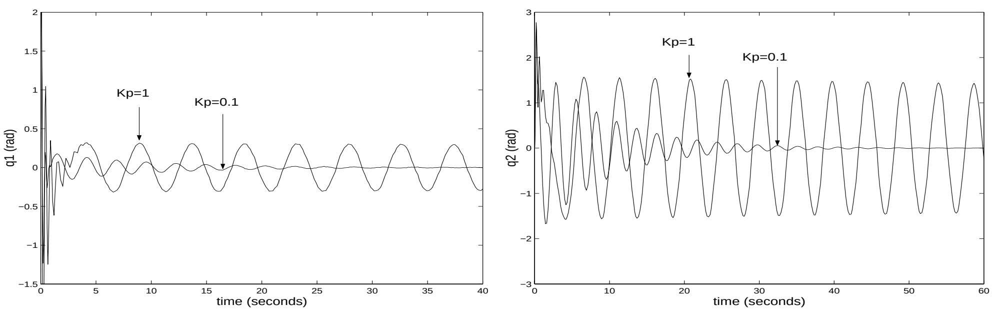

Figure 2: Evolution of $q_1(t)$ (left) and $q_2(t)$ for different values of k_p, letting $k_v = 10$

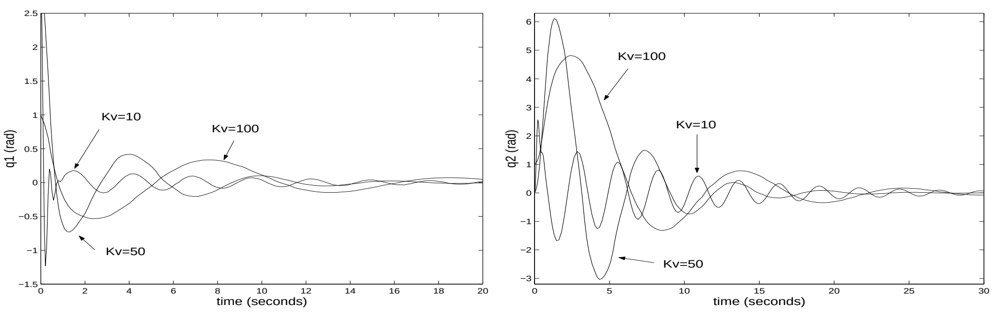

Figure 3: Evolution of $q_1(t)$ (left) and $q_2(t)$ for different values of k_v, and $k_p = 0.1$

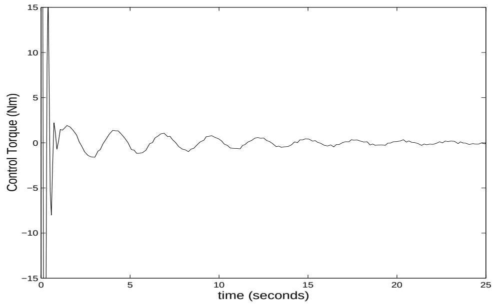

Figure 4: Control signal for $k_v = 10$, and $k_p = 0.1$

6 The Ball and Beam System

In this section we will design an IDA–PBC for the well–known ball and beam system depicted in Fig. 5. First, we will prove that for all initial conditions (except a set of zero measure) we drive the beam to the right orientation. Then, we define a domain of attraction for the zero equilibrium that ensures that the ball

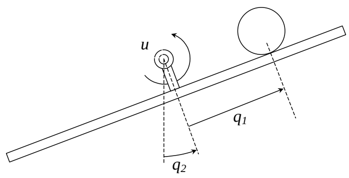

Figure 5: Ball and Beam System.

6.1 Model

The dynamic behavior of the ball and beam system, under time scaling and some assumptions on mass constants for simplicity, is described by the EL equations

$$\begin{aligned} \ddot{q}_1 + g\sin(q_2) - q_1\dot{q}_2^2 &= 0 \\ (L^2 + q_1^2)\ddot{q}_2 + 2q_1\dot{q}_1\dot{q}_2 + gq_1\cos(q_2) &= u \end{aligned} \tag{6.1}$$

where q_1, q_2 are the ball position and the bar angle, respectively,[16] and L is the length of the bar. Since we are interested in ensuring that the ball remains in the bar, we have explicitly included L in the model. We refer the reader to [14] for further details on the model. The Hamiltonian model (2.1), (2.2) is obtained defining the matrices

$$M(q_1) = \begin{bmatrix} 1 & 0 \\ 0 & L^2 + q_1^2 \end{bmatrix}, \; G = \begin{bmatrix} 0 \\ 1 \end{bmatrix}$$

and the potential energy function $V(q) = gq_1\sin(q_2)$. The control objective is to stabilize the ball and beam in its rest position with $q_{1*} = q_{2*} = 0$.

[16] The *caveat* of Subsection 5.1 applies here as well. Indeed, the model can be seen either as a system defined over $I\!R^4$ or over $I\!R \times \mathcal{S} \times I\!R^2$.

6.2 Controller Design

For pedagogical reasons, we will split now the design of the IDA-PBC into kinetic energy shaping, potential energy shaping, asymptotic stability and transient performance analysis.

A. Kinetic Energy Shaping

First, notice that M is a function of q_1 only, hence it is reasonable to propose M_d of the form (5.2), but with the coefficients a_1, a_2, a_3 *functions* (to be defined) of q_1 also. We will denote

$$J_2(q,p) = \begin{bmatrix} 0 & j(q,p) \\ -j(q,p) & 0 \end{bmatrix}$$

with the function j also to be defined.

Since this is the scenario of [10] discussed in Section 4 we apply directly the formula (4.1), with $G^\perp = [1\ 0]$, to derive the ODE's for M_d. This leads to the system of ODE's

$$\begin{aligned} \frac{d}{dq_1} a_1(q_1) &= \frac{2q_1}{(L^2+q_1^2)^2} \frac{a_2^2}{a_1} \\ \frac{d}{dq_1} a_2(q_1) &= \frac{2q_1}{(L^2+q_1^2)^2} \frac{a_2 a_3}{a_1} \end{aligned}$$

that has to be solved for a_1, a_2, and we view a_3 as a "free" parameter. To obtain two equations with two unknowns, we fix $a_3 = a_2 a_1$, hence we can easily get explicit solutions of the ODE's as

$$a_1 = \sqrt{2(\kappa + q_1^2)}, \qquad a_2 = L^2 + q_1^2 \tag{6.2}$$

with κ a free integration constant that must be chosen to ensure that M_d is positive definite. It is clear that $a_1 > 0$ for all $\kappa > 0$, furthermore the determinant of M_d results

$$a_3 a_1 - a_2^2 = \left(L^2 + q_1^2\right)\left(q_1^2 + 2\kappa - L^2\right)$$

which is positive, as desired, for all $\kappa > \frac{L^2}{2}$. For simplicity, we will take $\kappa = L^2$ in the sequel. The resulting M_d is then

$$M_d = (L^2 + q_1^2) \begin{bmatrix} \sqrt{2}(L^2+q_1^2)^{-1/2} & 1 \\ 1 & \sqrt{2(L^2+q_1^2)} \end{bmatrix} \tag{6.3}$$

The kinetic energy shaping is completed evaluating j from (2.11) and the M_d calculated above

$$j = q_1 \left[p_1 - \sqrt{2}(L^2+q_1^2)^{-1/2} p_2\right] \tag{6.4}$$

B. Potential Energy Shaping

Once we have determined the desired inertia and interconnection matrices we proceed now to define the closed–loop potential energy from the solution of (2.12), which in this case is expressed as

$$a_1(q_1)\frac{\partial V_d}{\partial q_1}(q) + \frac{a_2(q_1)}{L^2+q_1^2}\frac{\partial V_d}{\partial q_2}(q) = g\sin(q_2) \tag{6.5}$$

Substituting the solutions obtained for a_1 and a_2 in (6.2) yields

$$\sqrt{2(L^2+q_1^2)}\frac{\partial V_d}{\partial q_1}+\frac{\partial V_d}{\partial q_2}=g\sin(q_2)$$

We will solve this PDE using the symbolic language Maple. To help Maple find a suitable solution we introduce the change of coordinates $x_1=\frac{1}{L}q_1$, $x_2=q_2$, the PDE can then be rewritten as

$$a\sqrt{1+x_1^2}\frac{\partial V_d}{\partial x_1}(x)+b\frac{\partial V_d}{\partial x_2}(x)=\sin(x_2)$$

where we have defined $a\triangleq\frac{\sqrt{2}}{g}$ and $b\triangleq\frac{1}{g}$. The required Maple commands are

```
>equ:=a*diff(Vd(x1,x2),x1)*sqrt(1+x1\^2)+b*diff(Vd(x1,x2),x2)=sin(x2);
>sol:=pdsolve(equ);
```

which produces (after transforming back the coordinates)

$$\begin{aligned} V_d(q) &= -g\cos(q_2)+\Phi\left(z(q)\right) \\ z(q) &\triangleq q_2-\frac{1}{\sqrt{2}}\text{arcsinh}\left(\frac{q_1}{L}\right) \end{aligned}$$

with Φ an arbitrary differentiable function of z. This function must be chosen to ensure the equilibrium assignment, i.e., to satisfy (2.4) with $q_*=0$. Towards this end, let us evaluate the gradient

$$\nabla_q V_d(q)=\begin{bmatrix} \frac{-1}{\sqrt{2(L^2+q_1^2)}}\nabla_z\Phi(z(q)) \\ g\sin(q_2)+\nabla_z\Phi(z(q)) \end{bmatrix}$$

Clearly, a necessary and sufficient condition to assign the zero equilibrium is $\nabla_z\Phi(z(0))=0$. Remark that, independently of the choice of Φ, (or the integration constant κ), the closed–loop has other equilibrium points. Indeed, since $z(0)=0$ and $\sinh(\cdot)$ is an increasing first–third quadrant function, $\nabla_q V_d(\bar{q})=0$ has a countable number of roots given by $\bar{q}=(L\sinh(\sqrt{2}i\pi),i\pi)$, with $i\in I\!N$. On the other hand, we have that the only equilibrium with $|\bar{q}_1|\leq L$ is the zero equilibrium. Of course, this property is practically meaningful only if we can show that the trajectories $|q_1(t)|\leq L$ for all $t\geq 0$, which will be done later.

It is important to recall that, the equilibria $\bar{q}_2=i\pi$ with i even correspond to the bar in its original orientation, while for i odd the bar is rotated 180°. We will prove now that, with a suitable choice of Φ, we can make the former equilibria stable and the latter ones unstable.

To study the stability of the equilibria we check positivity of the Hessian of V_d, evaluated a $\bar{q}$, which yields

$$\nabla_q^2 V_d(\bar{q})=\begin{bmatrix} \frac{1}{2(L^2+\bar{q}_1^2)}\nabla_z^2\Phi(z(\bar{q})) & -\frac{1}{\sqrt{2(L^2+\bar{q}_1^2)}}\nabla_z^2\Phi(z(\bar{q})) \\ -\frac{1}{\sqrt{2(L^2+\bar{q}_1^2)}}\nabla_z^2\Phi(z(\bar{q})) & g\cos(\bar{q}_2)+\nabla_z^2\Phi(z(\bar{q})) \end{bmatrix}$$

Taking into account that $\cos(\bar{q}_2)=\pm 1$, depending on whether the bar is at its original position or rotated 180°, the determinant of this matrix is $\pm\frac{g}{2(L^2+\bar{q}_1^2)}\nabla^2\Phi(z(\bar{q}))$, and stability (instability) of the equilibrium is determined by the sign of $\nabla^2\Phi(z(\bar{q}))$. We then choose $\Phi(z)=\frac{k_p}{2}z^2$, with $k_p>0$. In this way, the equilibria corresponding to the bar in its original orientation will be stable, while the ones with the rotated bar are unstable.

The new potential energy takes the final form

$$V_d=g[1-\cos(q_2)]+\frac{k_p}{2}\left[q_2-\frac{1}{\sqrt{2}}\text{arcsinh}\left(\frac{q_1}{L}\right)\right]^2 \tag{6.6}$$

where we have added a constant to shift the minimum to zero. See Fig. 6.

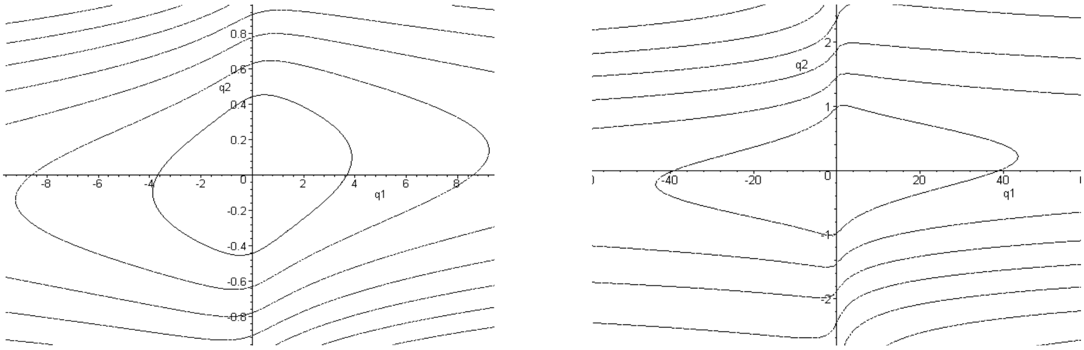

Figure 6: Level curves of $V_d(q)$ around the origin for $k_p = 0.05$ (left) and $k_p = 0.01$ (right).

C. Asymptotic Stability Analysis

To compute the final control law we first determine the energy–shaping term u_{es} from (2.10), which in this case takes the form

$$u_{es} = \nabla_{q_2} H - (M_d M^{-1})_{(2,1)} \nabla_{q_1} H_d - (M_d M^{-1})_{(2,2)} \nabla_{q_2} H_d + (J_2 M_d^{-1})_{(2,1)} p_1 + (J_2 M_d^{-1})_{(2,2)} p_2$$

Replacing the functions derived above for M_d and j, and after some straightforward calculations, we obtain the expression

$$u_{es} = \frac{q_1}{\sqrt{2}(L^2 + q_1^2)} \left[-\sqrt{L^2 + q_1^2}\, p_1^2 + \sqrt{2} p_1 p_2 + \frac{1}{\sqrt{L^2 + q_1^2}} p_2^2 \right] + \xi(q) \tag{6.7}$$

where

$$\xi(q) \triangleq g q_1 \cos q_2 - g\sqrt{2(L^2 + q_1^2)} \sin q_2 - k_p \sqrt{\frac{L^2 + q_1^2}{2}} \left(q_2 - \frac{1}{\sqrt{2}} \text{arcsinh}\left(\frac{q_1}{L}\right)\right)$$

The controller design is completed with the damping injection term (2.7), which yields

$$u_{di} = \frac{k_v}{L^2 + q_1^2} \left(p_1 - \sqrt{\frac{2}{L^2 + q_1^2}} p_2 \right) \tag{6.9}$$

It is important to underscore that, in spite of its apparent complexity, the controller is globally defined and its highest degree is quadratic. This is an important property of the control, since saturation should be avoided in all practical applications. Also, the role of the tuning parameters has a clear interpretation, namely: k_p is a *bona fide* proportional gain in position, as it multiplies terms that grow linearly in q, and k_v injects damping along a specified direction of velocities. Commissioning of the controller is simplified by this feature, as will be illustrated later in the simulations.

We give now a first result on asymptotic stability, similar to the one obtained for the inertia wheel pendulum, but with the fundamental difference that convergence to zero of the *ball* is only local. A more practical result, that takes into account the finite length of the bar, will be reported in the next subsection.

Proposition 4 *Consider the ball and beam model (6.1) in closed-loop with the static state feedback IDA–PBC* $u = u_{es} + u_{di}$*, with (6.7)–(6.9), and* $k_p, k_v > 0$*. Then, the origin is an asymptotically stable equilibrium with domain of attraction* $\Omega_{\bar{c}}$ *where* $\Omega_{\bar{c}} \triangleq \{(q,p) \in I\!R^4 \mid H_d(q,p) \leq \bar{c}\}$*, with* H_d

of the form (2.3), M_d given by (6.3), and V_d and $\bar{c}$ defined by (6.6), (2.8), respectively. Further, for all initial conditions, except a set of zero measure, the beam will asymptotically converge to its zero orientation position, i.e., for "almost" all trajectories $\lim_{t\to\infty} q_2(t) = 0$.

Proof. Stability of the zero equilibrium follows verifying the conditions of Proposition 1, however, to establish asymptotic stability, instead of checking detectability, we invoke Matrosov's theorem—see, e.g., Theorem 5.5 of [25]. For which we pick an auxiliary function $W(q) = q_1 + q_2$ whose derivative along the trajectories of the closed loop is

$$\dot{W} = p_1 + \frac{1}{L^2 + q_1^2} p_2$$

Now, $\dot{H}_d = 0$ if and only if

$$p_1 = \sqrt{\frac{2}{L^2 + q_1^2}} p_2$$

see (6.9), which (as q_1 ranges in $(-\infty, \infty)$) defines a triangular sector inside the first–third quadrant of the plane $p_1 - p_2$. On the other hand, the sector where $\dot{W} = 0$ lives in the second–fourth quadrant, consequently, we have that $\dot{W}$ is a non–vanishing definite function at the set $\{(q,p) | \dot{H}_d = 0\}$, and the conditions of the theorem are satisfied (in a neighborhood of zero) with H_d the required Lyapunov function.

Similarly to the proof of Proposition 2, to prove the "almost" convergence property stated above we look at the system in $I\!\!R \times \mathcal{S} \times I\!\!R^2$ to establish boundedness of all trajectories. To immerse the system in this cylinder we change the first coordinate to

$$\tilde{q}_1 = q_2 - \frac{1}{\sqrt{2}} \operatorname{arcsinh}\left(\frac{q_1}{L}\right) \tag{6.10}$$

and define accordingly the energy function

$$\tilde{H}_d(\tilde{q}_1, q_2, p) \triangleq \frac{1}{2} p^\top \tilde{M}_d^{-1}(\tilde{q}_1, q_2) p + \tilde{V}_d(\tilde{q}_1, q_2) \tag{6.11}$$

$$\tilde{V}_d(\tilde{q}_1, q_2) \triangleq g(1 - \cos q_2) + \frac{k_p}{2} \tilde{q}_1^2 \tag{6.12}$$

which is proper and positive definite in $I\!\!R \times \mathcal{S} \times I\!\!R^2$, and with negative semidefinite derivative. This proves boundedness of *all* trajectories in $I\!\!R \times \mathcal{S} \times I\!\!R^2$. The remaining of the proof mimics the one done for the inertia wheel pendulum, noting that for all stable equilibria we have the desired asymptotic behavior for q_2, while the other equilibria are unstable. $\triangleleft$

Before closing this section we note that in this example it is not possible to replace the measurements of velocities by its dirty derivative approximation as done for the inertia wheel. This stems from the fact that in the ball and beam controller, besides the damping injection term, the energy shaping term depends explicitly on p.

D. Transient Performance

It has been stated in Proposition 4 that in closed loop the origin is an asymptotically stable equilibrium with Lyapunov function the desired total energy. In this subsection we will refine this analysis, studying the effect of the tuning parameter k_p on the size of the domain of attraction, and explicitly quantifying a set of initial conditions such that the ball remains all the time in the bar, that is, $|q_1(t)| \le L$ for all $t \ge 0$.

First, we note that as H_d decreases and the kinetic energy is non–negative, we have that $V_d(q(t)) \leq H_d(q(0), p(0))$, hence the sub–level sets of V_d are invariant sets for $q(t)$. Further, if we can show that the kinetic energy is bounded, then the bounded sets provide an estimate of the domain of attraction. To study these sets we find convenient to work in the coordinates $(\tilde{q}_1, q_2, p_1, p_2)$, where $\tilde{q}_1$ was introduced in (6.10).[17] In these coordinates the potential energy function becomes (6.12)—which has the same analytical expression as the total energy of the simple pendulum—and the associated sub–level sets, i.e., $\{(\tilde{q}_1, q_2) \mid \tilde{V}_d(\tilde{q}_1, q_2) \leq c\}$, are of the form shown in Fig 7. We are interested here in the bounded connected components that contain the origin, that we will denote Ξ_c.

The following basic lemma will be instrumental in the sequel.

Lemma 1 *The set Ξ_c is bounded if and only if $c < 2g$.*

Proof. The fact that all elements $\tilde{q}_1$ in Ξ_c are bounded for all finite c is obvious, as $\frac{k_p}{2}\tilde{q}_1^2 \leq c - g(1 - \cos q_2)$. Hence, we can concentrate only on boundedness of q_2.

($\Leftarrow$) We have the following implication

$$\tilde{V}(\tilde{q}_1, q_2) < c \Rightarrow \cos(q_2) > 1 - \frac{c}{g} > -1$$

where we have used the positivity of k_p in the first right hand side inequality and $c < 2g$ to obtain the second one. Note that the strict inequality excludes an interval around $q_2 = \pi$ and $q_2 = -\pi$ from Ξ_c. This proves that $\Xi_c \subset \{(\tilde{q}_1, q_2) \mid q_2 \in (-\pi, \pi)\}$, and consequently q_2 is bounded.

($\Rightarrow$) Necessity will be proved by contradiction. For, we suppose that $c \geq 2g$. Then, it is clear that $\Xi_c \supset \{(\tilde{q}_1, q_2) \mid \tilde{q}_1 = 0\}$, which is an unbounded set, and consequently q_2 is unbounded. ◁

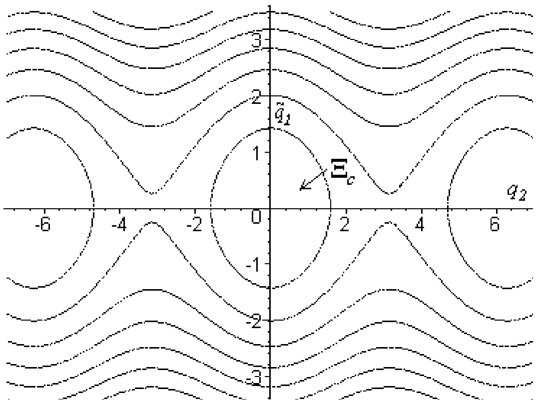

Figure 7: Level curves of $\tilde{V}(\tilde{q}_1, q_2)$.

We are in position to present the main result of this section. To simplify the notation we will use $(\cdot)^o$ to denote the value of the functions at $t = 0$.

Proposition 5 *Consider the ball and beam model (6.1) in closed-loop with the static state feedback IDA–PBC $u = u_{es} + u_{di}$, with (6.7)–(6.9), and $k_v > 0$.*

(i) We can compute a constant $k_p^M > 0$, function of the initial conditions (q^o, p^o), such that for all $k_p \leq k_p^M$, the set

$$\{(q, p) \mid \frac{1}{2} p^\top M_d^{-1}(q) p + g(1 - \cos q_2) < 2g\} \tag{6.13}$$

[17] Note that the coordinate mapping $(q_1, q_2) \mapsto (\tilde{q}_1, q_2)$ defines a global diffeomorphism, and recall that boundedness of sub–level sets is invariant under the action of diffeomorphisms.

is an estimate of the domain of attraction of the zero equilibrium. In particular, all trajectories starting with zero velocity, and $q_2^o \in (-\pi, \pi)$ *will asymptotically converge to the origin.*

(ii) Fix $k_p \leq k_p^M$ *and assume* $|q_1^o| < L$*. Then,*

$$\{(q,p) \mid \frac{1}{2}p^\top M_d^{-1}(q)p + g(1-\cos q_2) + \frac{k_p}{2}\left(q_2 - \frac{1}{\sqrt{2}}\text{arcsinh}\left(\frac{q_1}{L}\right)\right) < \frac{1}{8}\frac{k_p g}{2k_p+g}\} \quad (6.14)$$

is a domain of attraction of the zero equilibrium, such that all trajectories starting in this set satisfy $|q_1(t)| < L$ *for all* $t \geq 0$*.*

Proof. We have shown above that the sub–level sets of $V_d(q)$ are invariant sets for $q(t)$. Further, Lemma 1 establishes that the connected component of the sub–level sets of $V_d(q)$ containing the origin is bounded if and only if $c < 2g$. Hence, setting $c = H_d^o$ in Lemma 1 it follows that this set is bounded if and only if

$$H_d^o = \frac{1}{2}(p^o)^\top M_d^{-1}(q^o)p^o + g(1-\cos(q_2^o)) + \frac{k_p}{2}\tilde{q}_1^2 < 2g$$

It is clear that, if the first two terms are strictly smaller than g, we can always find and upperbound on k_p such that the inequality holds. To complete the proof of point (i) of the proposition we remark that, for all trajectories starting in the set (6.13), $q(t)$ is bounded. Hence, from (5.2), we conclude that $M_d^{-1}(q(t)) > \epsilon I$ from some constant $\epsilon > 0$. This, together with the fact that $\frac{1}{2}p^\top(t)M_d^{-1}(q(t))p(t) < H_d^o$, establishes that the corresponding $p(t)$ is also bounded and the set (6.13) is an estimate of the domain of attraction.

The proof of (ii) proceeds as follows. From (6.10) we have that

$$|q_1| \leq L \Leftrightarrow |q_2 - \tilde{q}_1| \leq \frac{1}{\sqrt{2}}\text{arcsinh}(1) \quad (6.15)$$

where we have used the fact that arcsinh(·) is odd and monotonic. The region defined by (6.15) is depicted in Fig. 8 together with two sets Ξ_c. Our problem is then to compute the largest c such that the set Ξ_c does not intersect the lines $\tilde{q}_1 = q_2 \pm \frac{1}{\sqrt{2}}\text{arcsinh}(1)$. To simplify the expressions we note that $\frac{1}{\sqrt{2}}\text{arcsinh}(1) > \frac{1}{2}$, and check the intersection with the "closer" lines $\tilde{q}_1 = q_2 \pm \frac{1}{2}$ in the band $q_2 \in [-\frac{1}{2}, \frac{1}{2}]$. For, we substitute $\tilde{q}_1 = q_2 + \frac{1}{2}$ in the boundary equation of Ξ_c, and use the bound $\cos q_2 < 1 - \frac{q_2^2}{4}$, which is valid in the aforementioned band, to get the first inequality below

$$g(1-\cos q_2) + \frac{k_p}{2}\left(q_2 + \frac{1}{2}\right) > g\frac{q_2^2}{4} + \frac{k_p}{2}\left(q_2 + \frac{1}{2}\right) > c$$

The second inequality holds for all $c < \frac{1}{8}\frac{k_p g}{2k_p+g}$ and all q_2 in the band. This proves that the boundary of Ξ_c does not intersect the limit lines within the band. They cannot intersect outside the interval either because $c > g(1-\cos(\frac{1}{2}))$ implies that, in Ξ_c, $|q_2| < \frac{1}{2}$, and this bound on c is less strict than $c < \frac{1}{8}\frac{k_p g}{2k_p+g}$. This completes the proof.

◁

6.3 Simulations

A set of simulations of the ball and beam system with $g = 9.8$, $k_p = 1$ has been made. The results are shown in Fig. 9. The graphs on the upper row depict the ball position q_1 and the beam angle

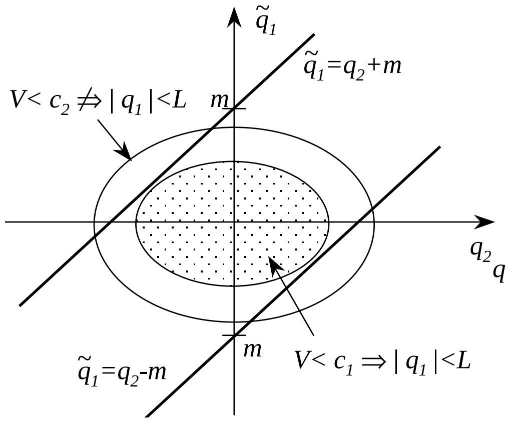

Figure 8: Graphical interpretation of $|q_1| < L$, with $m \triangleq \frac{1}{\sqrt{2}}\text{arcsinh}(1)$.

q_2 for zero initial velocity, and varying initial positions and parameters. Under each of these, the corresponding graphs with the desired hamiltonian H_d and potential energy V_d are shown. Each column in the graph array belongs to a single simulation. From the first two simulations we see the effect of increasing the damping constant k_v starting with the bar in vertical position. Note that the convergence is not always accelerated with higher values of k_v, as new oscillations come into play. The third simulation starts at rest with the bar in horizontal position and the ball on the edge of the bar. Apparently, the controller works best starting from $q_2(0) = 0$. To ensure that the initial condition is within the domain of attraction, k_p has been chosen smaller than k_p^M according to Proposition 5. Figure 9 also illustrates the monotonic nature of H_d together with the fact that $V_d(t) < H_d(t) < H_d(0)$ for all t.

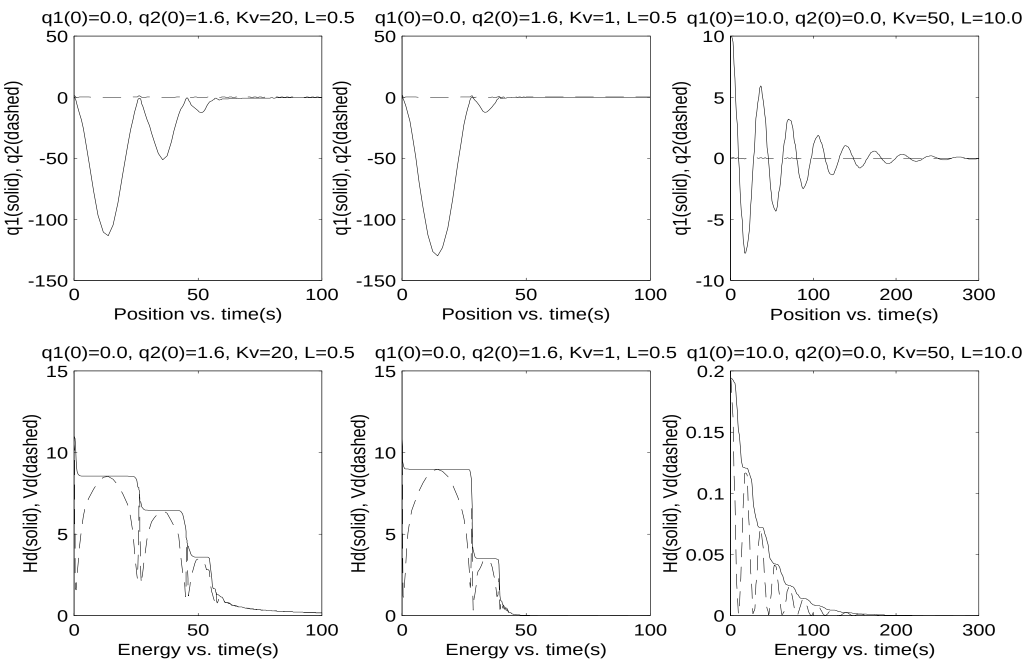

Figure 9: Simulations of the ball and beam starting from rest.

The effect of the limited bar length and the use of the last part of Proposition 5 is illustrated by simulation in Fig. 10. The parameters are $g = 9.8$, $k_p = 1$, $k_v = 50$, and $L = 10$. Hence the condition for keeping the ball within the limits of the bar is $H_d(0) < 0.1038$. The first simulation starts at $(q^0, p^0) = (8, 0, 1, 1)$ with $H_d(0) = 0.1837$. Due to the initial velocity the controller is unable to *catch* the ball before it trespasses the limit of the bar ($L = 10$). In the second simulation we have $(q^0, p^0) = (6, 0, 0.5, 1)$ and $H_d(0) = 0.0928$, thus the bound $|q_1| < L$ is guaranteed and the ball remains within the limits of the bar.

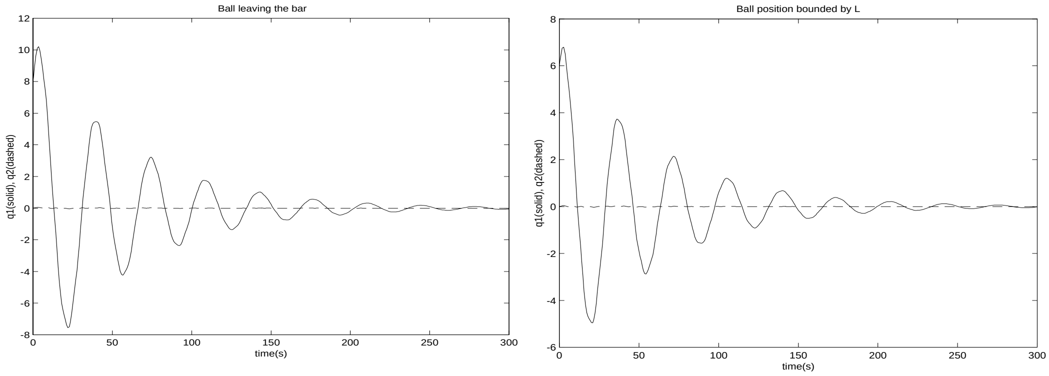

Figure 10: Ball and beam starting with initial velocity. Effect of the finite bar length.

7 Conclusions

We have characterized in this paper a class of underactuated mechanical systems for which the newly developed IDA–PBC design methodology yields smooth stabilization. The class is given in terms of solvability of two PDE's (2.11), (2.12). Although it is well–known that solving PDE's is in general hard, we have added some degrees of freedom—the closed–loop interconnection J_2—to simplify this task.

As an illustration we have presented a dynamic nonlinear output feedback IDA–PBC which stabilizes for all initial conditions (except a set of zero measure) the upward position of a novel inverted pendulum. We believe this is the first result of swinging up and balancing an underactuated pendulum without switching nor measurement of velocities. See also [22] for an alternative, full–state feedback, solution using a variation of forwarding. We have also derived a static state–feedback IDA–PBC for the well–known ball–and–beam system, which asymptotically stabilizes the zero equilibrium for a well-defined set of initial conditions, maintaining the ball inside the length of the bar. Again, to the best of the authors' knowledge, no similar transient performance result is available in the literature. Current research is under way to test these controllers experimentally.

There are many possible extensions of the work reported here. First, to by–pass the need to solve the (infamous) PDE's we can dualize the problem, fixing the energy function H_d to some desired form, and trying to solve the resulting algebraic equation for J_d. This is, in essence, the approach adopted in the recent paper [9], see also [24]. Second, we discussed in Section 3 that IDA–PBC allows the consideration of gyroscopic forces in the energy function. Although it is not clear at this stage how can this be profitably used in mechanical applications, they play a fundamental role in electromechanical applications, where the desired equilibrium does not occur at zero kinetic energy. Some preliminary results along these lines for magnetic levitated systems and electric motors are very encouraging [24]. Third, it would be, of course, desirable to have a better understanding of the PDE's appearing in IDA–PBC, on one hand, to obtain a more systematic design procedure, and on the other hand, to come to terms with the intrinsic limitations of the methodology (e.g., deriving conditions for (non)solvability of the PDE's.) Some available results, and open research lines, in this direction are discussed in Section 4. A particularly important aspect is that, for stability purposes, it is not enough to find any solution M_d and V_d of the PDE's, but we need one that satisfies some kind of "boundary conditions". The study of this additional constraint is essentially open.

Acknowledgements

The authors express their gratitude to the anonymous reviewers for many helpful remarks. We are also greatful to the authors of [2] and [7] for providing us an advanced copy of their papers. Part of this work was carried out while the first author was visiting the University of Illinois. The hospitality of this institution is gratefully acknowledged. He would also like to thank Laurent Praly of Ecoles des Mines, Paris, and Diego Alonso and Eduardo Paolini of the Universidad del Sur, Bahia Blanca, for many helpful discussions. The work of Fabio Gómez-Estern and Guido Blankenstein was partly funded by the Research Network NACO-2 of the European Union.

References

[1] D. Auckly, L. Kapitanski and W. White, Control of nonlinear underactuated systems, *Comm. Pure Appl. Math.*, Vol. 3, 2000, pp. 354–369.

[2] D. Auckly and L. Kapitanski, On the λ–equations for matching control laws, *Preprint*, 2001.

[3] F. Andreev, D. Auckly, L. Kapitanski, S. Gosavi, A. Kelkar and W. White, Matching, linear systems, and the ball and beam, *Preprint*, 2000.

[4] G. Blankenstein, R. Ortega and A.J. van der Schaft, The matching conditions of controlled Lagrangians and interconnection assigment passivity based control, *LSS Int. Report*, April 2001. (To appear in *Int J of Control*.)

[5] A. Bloch, N. Leonard and J. Marsden, Controlled Lagrangians and the stabilization of mechanical systems, *IEEE Trans. Automat. Contr.*, Vol. 45, No. 12, December 2000.

[6] A. Bloch, D. Chang, N. Leonard and J. Marsden, Potential and kinetic shaping for control of underactuated mechanical systems, *Proc. ACC*, Chicago, IL, USA, June 2000, pp. 3913–3917.

[7] A. Bloch, D. Chang, N. Leonard, J. Marsden and J. Woolsey, The equivalence of controlled Lagrangian and controlled hamiltonian systems for simple mechanical systems, *Preprint*, June 29, 2001.

[8] C. Byrnes, A. Isidori and J.C. Willems, Passivity, feedback equivalence, and the global stabilization of minimum phase nonlinear systems, *IEEE Trans Aut. Cont.*, Vol.36, no.11, pp. 1228–1240, 1991.

[9] K. Fujimoto and T. Sugie, Stabilization of Hamiltonian systems with nonholonomic contraints based on time–varying generalized canonical transformations, *Systems and Control Letters*, Vol. 44, No. 15, pp. 309–320, 2001.

[10] F. Gomez-Estern, R. Ortega, F. Rubio and J. Aracil, Stabilization of a class of underactuated mechanical systems via total energy shaping, *IEEE Conf on Decision and Control*, Orlando, FL, USA Dec. 4–7, 2001.

[11] F. Gomez-Estern, R. Ortega and M.W. Spong, Total Energy Shaping for Underactuated Mechanical Systems *5th IFAC Symp. Nonlinear Control Systems, NOLCOS'01*, St Petersburg, Russia, July 4–6, 2001.

[12] J. Hamberg, Controlled lagrangians, symmetries and conditions for strong matching, *Proc. IFAC Workshop on Lagrangian and Hamiltonian Methods for Nonlinear Control*, eds. N. Leonard and R. Ortega, March 16–18, 2000, Princeton, NJ, USA, pp. 62–67.

[13] J. Hamberg, Generalized matching conditions in the theory of controlled lagrangians, *Proc. 38th IEEE Conf. Decision and Control*, Phoenix, AZ, USA, Dec. 7–10, 1999, pp. 2519–2523.

[14] J. Hauser, S. Sastry, and P. Kokotović, Nonlinear control via approximate input-output linearization: the ball and beam example, *IEEE Transactions on Automatic Control*, Vol. 37, No. 3 March 1992, pp. 392-398.

[15] R. Kelly, A simple set point robot controller by using only position measurements, *Proc. 12th IFAC World Conf.*, Vol. 6, pp. 173–176, Sydney, Australia, 1993.

[16] R. Ortega, A. Loria, P. J. Nicklasson and H. Sira–Ramirez, **Passivity–based control of Euler–Lagrange systems**, Springer-Verlag, Berlin, Communications and Control Engineering, Sept. 1998.

[17] R. Ortega, A. Loria, R. Kelly and L. Praly: On output feedback global stabilization of Euler-Lagrange systems, *Int. J. of Robust and Nonlinear Cont.*, Special Issue on Mechanical Systems, Eds. H. Nijmeijer and A. van der Schaft, Vol. 5, No. 4, pp. 313-324, July 1995.

[18] R. Ortega, A. van der Schaft, B. Maschke and G. Escobar, Stabilization of port-controlled hamiltonian systems: energy-balancing and passivation, *Automatica*, (to appear). See also: *Stability and stabilization of nonlinear systems*, LNCIS Vol. 246, eds. D. Aeyels, F. Lamnabhi–Lagarrigue and A. van der Schaft, Springer–Verlag, London, 1999.

[19] R. Ortega, A. van der Schaft, I. Mareels and B. Maschke, Putting energy back in control, *IEEE Control Syst. Magazine*, Vol. 21, No. 2, April 2001, pp. 18–33.

[20] R. Ortega and M. Spong, Adaptive motion control of rigid robots: A tutorial, *Automatica*, Vol. 25, No.6, pp. 877-888, 1989.

[21] R. Ortega and M. Spong: Stabilization of underactuated mechanical systems via interconnection and damping assignment, *Proc. IFAC Workshop on Lagrangian and Hamiltonian methods in nonlinear systems*, pp. 74–79, Princeton, NJ, March 16–18, 2000.

[22] L. Praly, R. Ortega and G. Kaliora, Stabilization of nonlinear systems via forwarding $mod\{L_gV\}$, *IEEE Transactions on Automatic Control*, Vol. AC–46, No. 9, Sept. 2001.

[23] M. Reyhanoglu, A. van der Schaft, N. McClamroch and I. Kolmanovsky, Dynamics and control of underactuated mechanical systems, *IEEE Trans. Automat. Contr.*, Vol. 44, N0. 9, Sept. 1999, pp. 1663–1671.

[24] H. Rodriguez and R. Ortega, Interconnection and damping assignment control of electromechanical systems, *15th World IFAC'99*, Barcelone, Spain, 21–26 July, 2002. (Submitted.)

[25] N. Rouche and J. Mawhin, **Ordinary Differential Equations: Vol II**, Pitman Publ., London, 1980.

[26] A. Shiriaev, et al., On global properties of passivity-based control of the inverted pendulum, *Int J of Robust and Nonlinear Control*, Vol. 10, No. 4, 2000, pp. 283–300.

[27] M.W. Spong and M. Vidyasagar, **Robot Dynamics and Control**, John Wiley & Sons, Inc., New York, 1989.

[28] A. J., van der Schaft, L_2–**Gain and Passivity Techniques in Nonlinear Control**, Springer-Verlag, Berlin, 1999.

[29] Krstić, M., Sepulchre, R., Praly, L. On the measure of global invariant manifold for fixed points, *Technical Report CCEC 95-0228,* University of California, Santa Barbara, February 1995.